Electrodeposition, synthesis of ZnO Nanowires through AAMs

[1]Dr. Satish Kumar and [2]Sindhu Chauhan

[1]Assistant Professor, Department of Physics, OPJS University, Churu, Rajasthan (India)
[2]Research Scholar, Department of Physics, OPJS University, Churu, Rajasthan (India)
Email: sindhu17chauhan@gmail.com

Abstract: current vs time response for potentiostatic deposition of ZnO nanowires indicating four regions I, II, III and IV as explained earlier in the case of structure growth for CdS nanowires. It is difficult to determine the end of the synthesis, because no constant current is observed. For this reason, it is preferable to use smaller deposition currents in order to decrease the deposition rate, facilitating control over the process. The crystallanity of electrodeposited ZnO nanowires was confirmed by XRD studies which were carried out using X-ray diffractometer (PW1710) with Cu-Kα (λ = 1.54Å) radiation. The scanning was done between 20 degrees and 60 degrees for 2 theta values. The typical 2θ and d-values for different planes in ZnO nanowires. X-Ray diffraction pattern of ZnO nanowires. Strong reflections corresponding to (100), (002), (101), (102) and (110) are observed indicating that ZnO nanowires were polycrystalline in nature. From the XRD it is clear that (101) plane is more crystalline phase and structure of ZnO is wurtzite. Laser induced pulse excitation method was used to study the PL spectra of ZnO nanowires. The decay signals (5) from the ZnO nanowires were recorded by digital storage oscilloscope and analysed using computer simulations to calculate emission wavelength of the nanowires. The emission wavelength of ZnO nanowires is found to be 590 nm (2.1 eV). In photoluminescence spectra, a strong peak at 590 nm in the visible region is observed. The visible emission at 590 nm corresponds to deep level emission due to defects. This defect related emission is attributed to the single ionized oxygen vacancy in ZnO, and it results from radioactive recombination of electron related to oxygen vacancies and photogenerated holes (Vanheusden et al 1996). It is generally accepted that the defect related emission depends upon crystal quality –the better crystal quality enhances the UV-emission with reduction of the deep level emission (Umar et al 2006). In our case, the ZnO nanowires are polycrystalline in nature which shows that the appearance of visible peak at 590 nm in photoluminescence spectrum is consistent with the XRD investigations.

[Kumar, S. and Chauhan, S. **Electrodeposition, synthesis of ZnO Nanowires through AAMs.** *Academ Arena* 2019;11(8):18-22]. ISSN 1553-992X (print); ISSN 2158-771X (online). http://www.sciencepub.net/academia. 4. doi:10.7537/marsaaj110819.04.

Keywords: Electrodeposition, ZnO Nanowires, AAMs.

Introduction:

Electroplating process was used for the first time in the beginning of 19th century by Luigi Bugnatelli (1761-1817), a colleague of Alessandro Volta, the inventor of the Volta pile, for depositing gold on silver coin. Another milestone was reached around 1840 when Moritz Hermann Jacobi-a German Physicist and Engineer in Russia fabricated printing press plates used for printing of Russian Banknotes through acidic copper electroplating (http://chem.ch.huji.ac.il; www.artisanplating.com). Since then, this process has been widely used for surface finishing and precision forming. Important application of electroplating was done by IBM in late seventies by introducing through-mask plating of magnetic heads and in late nineties by replacing vapor deposited aluminium interconnects in computer chips by electrodeposited copper (www.ibm.com). Now a days, electroplating process is of fundamental importance in computer, electronics and micro-machines industries which are exhibiting a trend towards miniaturization (Datta and Landolt 2000, Lau 1996). Electroplating of Cu has been employed for interconnect fabrication in the next generation of sub-0.25 micron microelectronics devices (Hamakawa et al 1993) and electroplating of gold has been used in electronics industry for wide variety of applications (Datta et al 2005, Holliday and Paul 2002, Christie and Cameron 1994, Green 2007).

Electrodeposition finds a niche in depositing metals or alloys for microelectronic fabrication and high aspect ratio nano-/microstructures. The properties of interest for high aspect ratio nanostructures cover a broad range, including catalytic, electrical, magnetic and optical characteristics. The nano-/microstructures in the form of metallic whiskers, cylinders or wires fabricated through template synthesis via electrodeposition can be crystalline in nature (Dobrev et al 1995). Chakarvarti and Vetter (1993) have deposited Cu-Se heterojunctions through electrodeposition using track-etch templates and confirm the crystallinity through XRD spectrum. In the present work, we have synthesized CdS and ZnO nano-/ microstructures through electrodeposition using TEMs and AAMs as templates.

In order to deposit nano-/micro wires or nano-/micro tubules of metals (Tomassi and Buczko 1998; Whitney et al 1993; Penner and Martin 1987; Chakarvarti and Vetter 1991; Dobrev et al 1995; Tierney and Martin 1989), semiconductors (Enculescu et al 2005), metal–semiconductor heterojunctions (Chakarvarti and Vetter 1993), and conductive polymers (Lakshami et al 1997; DeVito and Martin 1998; Marinakos et al 1998; Nishizawa et al 1997; Wu and Bein 1994), electrodeposition can be done either galvanostatically or potentiostatically. In galvanostatic process, the current passing between anode and cathode is kept constant. In this mode of deposition, the cathode potential and consequently the chemical reaction occurring at the electrode may vary leading to hydrogen evolution. In potentiostatic deposition, the potential between the cathode and anode is kept constant so that the applied potential determines which reaction can take place and the current density can vary with time. The estimated amount of material deposited is determined by Faraday's law:

$I / n F = m / MW. t. \varepsilon$

Where I = current, n = number of electrons

F = Faraday's constant, MW = molecular weight

t = time for deposition, m = mass deposited,

andε = efficiency factor

In addition to low cost, easy scale up and maintenance, low operating temperatures, electrodeposition is the most efficient method over competing technologies such as physical or chemical vapour deposition (CVD) because it can overcome the geometrical constraints of inserting materials into very deep recesses such as in nanoporous templates.

The parameters such as inter-electrode distance, deposition potential, current density, standard composition of electrolytes etc affect electrodeposition process. It is also found that under the influence of an applied potential, the ions in the vicinity of the electrode surface are rearranged, resulting in the formation of Helmholtz layer which is further joined by diffusion layer. Thus the migration of metal ions in the bulk of electrolyte is towards the cathode. Some practical aspects of electroplating were discussed by Khera (1974). Electrodeposition of metals is not always possible even in case of reactive and more electronegative metals like aluminium, molybdenum, tungsten, titanium, zirconium and niobium. Electrodeposition of metals in corrosive electrolytes or electroplating of noble metals such as gold and silver on base metals needs much care due to poor adhesion. In case of nano-/microporous template, rinsing off the template with 3 % H_2SO_4, followed by distilled water and absolute ethyl alcohol would facilitate the galvanic process for depositing metals like zinc, indium etc. (Possin 1970). However, pre-soaking of the cleaned and washed template with given electrolyte is also helpful sometimes (Chakarvarti and Vetter 1991).

For applying deposition potential and monitoring the current and potential drop across the cell, good constant current/constant voltage power supplies and digital multimeters or electrometers are used. Sometimes, pulsating currents rather than direct or constant current is also useful. Davis and Podlaha (2004) have employed potentiostatic pulse for Co-Ni-Fe-Cu/Cu multilayered nanowires. The introduction of high initial current density for short duration followed by low current density produces good results. It is observed by number of researchers through current vs time plots that nano-/microwire growth is not a steady state process. Initially, when the pores of template are empty, the current drops suddenly and attains an almost steady state when wires start growing. With the pore filling advancement, current gradually increases and reaches a steady state when wires reach the top of the template. As during deposition the exposed area of membrane to be filled is constant, therefore, the resulting current is also constant. Sometimes over deposition appears either in the form of 'buds' or 'caps' (Vetter and Sphor 1993) or 'christmas tree' formation (Chakarvarti and Vetter 1998).

Synthesis of ZnO Nanowires through AAMs

ZnO nanowires have been fabricated by electrodeposition within the nano channels of AAMs (pore diameter-100 nm from Whatman, USA). In order to make the bottom surface of AAM conducting, a thin layer of gold ~ 50 nm thick was deposited by sputtering. The deposition cell used here for synthesis of ZnO nanowires is as shown earlier in figure 3.2. The cathode (Cu tape as substrate having its base coated with conductive adhesive) was covered closely with the AAM as an overlayed template and the electrolyte solution to be used in the bath was prepared using milliQ 10 MΩ water and ultra high purity reagents 0.05 M $ZnCl_2$ and 0.1 M KCL. The pH value of electrochemical bath was 6.85. The oxygen precursor used here was H_2O_2. Another precursors reported in literature are molecular oxygen, nitrate ions and H_2O_2 (Umar et al 2006 and refs. therein). The H_2O_2 is advantageous because it is highly soluble in aqueous medium and does not produce any by-product via reduction. The galvanic replication was carried out for 40 minutes at 1.5 V at a temperature of 70 ± 1^0C using pure zinc as anode. During deposition, the key reactions in the formation of ZnO nanowires arrays are the reduction of H_2O_2 to OH^- ions at the electrode surface:

$H_2O_2 + 2e^- \rightarrow 2\ OH^-$

and the precipitation of ZnO from the aqueous solution:

$Zn^{2+} + 2\ OH^- \rightarrow ZnO + H_2O$

The figure 1 shows the current vs time response for potentiostatic deposition of ZnO nanowires indicating four regions I, II, III and IV as explained earlier in the case of structure growth for CdS nanowires. It is difficult to determine the end of the synthesis, because no constant current is observed. For this reason, it is preferable to use smaller deposition currents in order to decrease the deposition rate, facilitating control over the process.

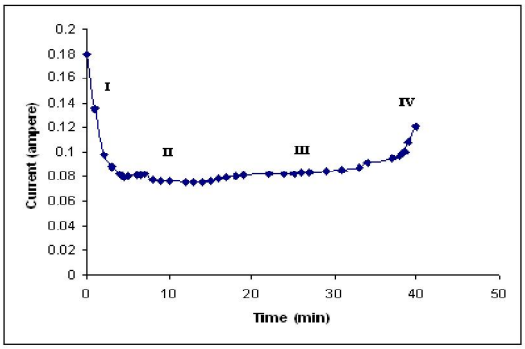

Fig. 1 Current response for potentiostatic deposition of ZnO

Morphological characterization of ZnO nanowires

After the plating process was over, the AAO template overlay along with the substrate was removed and the template was dissolved carefully in 1M NaOH solution for 30 minutes followed by rinsing with double distilled water so that the grown nanostructures with Cu as substrate or a platform were revealed. The cleaned and dried samples were imaged under SEM at an accelerating voltage of 10 kV. The figures 2 and 3 show the SEM photographs of ZnO nanowires which reveal that the nanowires were the true replica of pore geometry.

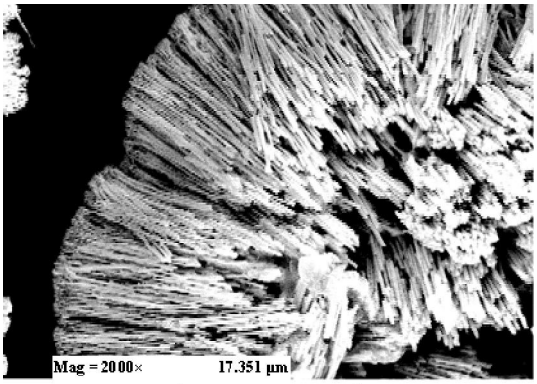

Fig. 2 SEM photograph of ZnO nanowires (100nm)

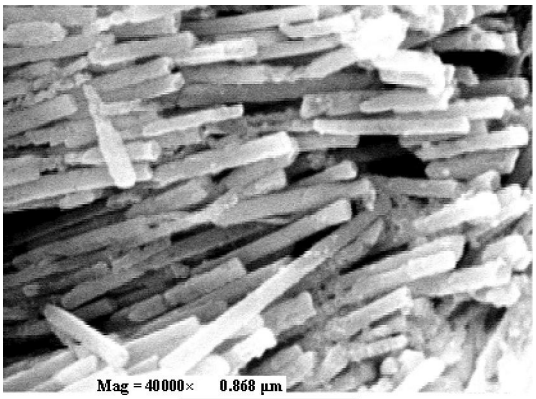

Fig. 3 Closer view of ZnO nanowires (100nm)

The crystallanity of electrodeposited ZnO nanowires was confirmed by XRD studies which were carried out using X-ray diffractometer (PW1710) with Cu-Kα (λ = 1.54Å) radiation. The scanning was done between 20 degrees and 60 degrees for 2 theta values. Table 1 shows the typical 2θ and d-values for different planes in ZnO nanowires. X-Ray diffraction pattern of ZnO nanowires is shown in figure 4. Strong reflections corresponding to (100), (002), (101), (102) and (110) are observed indicating that ZnO nanowires were polycrystalline in nature. From the XRD it is clear that (101) plane is more crystalline phase and structure of ZnO is wurtzite.

The mean crystallite size in ZnO nanowires is estimated from XRD peak width of (110) plane using Scherrer equation which is given by

$D = K\lambda / \beta \cos\theta,$

where K is constant (shape factor with approximate value 0.9); λ = 1.54 A^0, the wavelength of the x-ray used; β is the FWHM of the diffraction line, and θ is the Bragg's angle. The average crystallite size is found to be 22 nm.

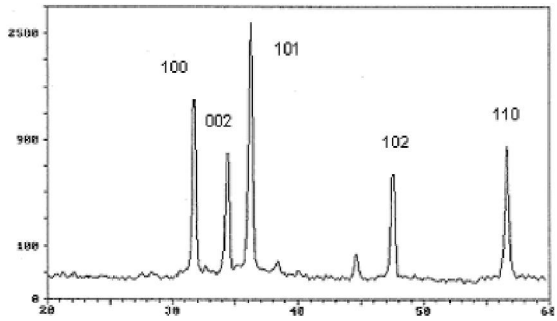

Fig. 4 XRD spectrum of ZnO nanowires (100nm)

Table 1 Typical 2θ and d-values for different plane in ZnO nanowires

Sample	Plane	2θ values	d-value (A^0)	Relative intensity
ZnO nano-wires	(100)	31.60	2.829	60.4
	(002)	34.25	2.616	42.9
	(101)	36.09	2.486	100.0
	(102)	47.38	1.917	20.7
	(110)	56.44	1.629	30.4

PL studies of ZnO nanowires

Laser induced pulse excitation method was used to study the PL spectra of ZnO nanowires. The decay signals (5) from the ZnO nanowires were recorded by digital storage oscilloscope and analysed using computer simulations to calculate emission wavelength of the nanowires. The emission wavelength of ZnO nanowires is found to be 590 nm (2.1 eV).

In photoluminescence spectra, a strong peak at 590 nm in the visible region is observed. The visible emission at 590 nm corresponds to deep level emission due to defects. This defect related emission is attributed to the single ionized oxygen vacancy in ZnO, and it results from radioactive recombination of electron related to oxygen vacancies and photogenerated holes (Vanheusden et al 1996). It is generally accepted that the defect related emission depends upon crystal quality –the better crystal quality enhances the UV-emission with reduction of the deep level emission (Umar et al 2006). In our case, the ZnO nanowires are polycrystalline in nature which shows that the appearance of visible peak at 590 nm in photoluminescence spectrum is consistent with the XRD investigations.

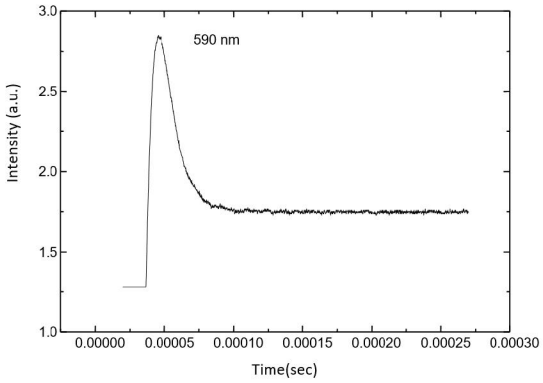

Fig 5 Photoluminescence spectra of ZnO nanowires

Correspondence address:
Sindhu Chauhan
Research Scholar, Department of Physics,
OPJS University, Churu, Rajasthan (India)
Email- sindhu17chauhan@gmail.com

References:

1. Becker M. F., J. R. Brock, H. Cai, N. Chaudhary, D. Henneke, L. Hilsz, J. W. Keto, J. Lee, W. T. Nichols, and H. D. Glicksman (1997), "*Nanoparticles generated by laser ablation*", In. Proc. of the Joint NSF-NIST Conf. on Nanoparticles.
2. Bercu B., I. Enculescu, and R. Sphor (2004), "*Copper tubes prepared by electroless deposition in ion track templates*", Nucl. Instr. And Meth. In Phys. Res. B225, 497-502.
3. Berndt C. C., J. Karthikeyan, T. Chraska, and A. H. King (1997), "*Plasma spray synthesis of nanozirconia powder*", In. Proc. of the Joint NSF-NIST Conf. on Nanoparticles.
4. Curulli A., F. Valentini, G. Padeletti, A. Cusma, G. M. Ingo, S. Kaciulis, D. Caschera, and G. Palleschi (2005), "*Gold nanotubules arrays as new materials for sensing and biosensing: Synthesis and characterization*", Sensors and actuators B 111-112, 526-531.
5. Datta M. and D. Landolt (2000), "*Fundamental aspects and applications of electrochemical microfabrication*", Electrochimica Acta 45, 2535-2558.
6. Datta M., T. Osaka and J. W. Schulze (Editors) (2005), "*Microelectronic packaging*", CRC Press, Boca Raton.
7. Davis D. and E. J. Podlaha (2004), "*CoFeNiCu/Cu nanowires and tubes*", 205th Meeting of the Electrochemical Society, San Antonio, TX.
8. De Heer W. A., W. S. Bacsa, A. Chatelain, T. Gerfin, R. Humphery-Baker, L. Forro, and D. Ugarte (1995), "Aligned *carbon nanotubes films: production and optical and electrical properties*", Science 268,845-847.
9. Feeney R. and S. P. Kounaves (2000), "*Microfabricated ultramicroelectrode arrays: developments, advances and applications in environmental analysis*", Electroanalysis 12, 9, 677-684.
10. Fendler J. H. (2001), "*Chemical Self assembly for electronics applications*", Chem. Mat. 13, 10, 3196-3210.
11. Fendler J. H. (2001a), "*Colloid chemical approach to nanotechnology*", Korean J Chem. Eng. 18, 1.

12. Ferain E. and R. Legras (2003), "*Track-etch templates designed for micro- and nanofabrication*", Nucl. Instr. and Meth., B208, 115-122.
13. Fernandes N. E., S. M. Fisher, J. C. Poshusta, D. G. Vlachos, M. Tsapatsis and J. J. Watkins (2001), "*Reactive deposition of metal thin films within porous supports from supercritical fluids*", Chem. Mater. 13, 2023.
14. Feynman R. P. (1960), "*There's Plenty of Room at the Bottom*", Engineering and Science 23, 5, 22-26.
15. Fischer B. E. and R. Sphor (1983), "*Production and use of nuclear tracks: Imprinting structures on solids*", Rev. Mod. Phys., 55, 4, 907-948.
16. Fischer B. E., M. Cholewa and H. Noguchi (2001), "*Some experiences on the way to biological single ion experiments*", Nucl. Instr. and Meth. B 181, 60-65.
17. Fleischer N., M. Genut, L. Rapoport, and R. Tenne (2003), "*New nanotechnology solid lubricants for superior dry lubrication*", European Space Agency (Special Publication) ESA SP 524, 65-66.
18. Hulteen J. C. and C. R. Martin (1997), "*A general template-based method for the preparation of nanomaterials*," J. Mater. Chem., 7, 7, 1075-1087.
19. Hyeon T., K. S. Suslik, and M. Fang (1996), "*Nanostructured molybdenum carbide: Sonochemical synthesis and catalytic properties*", J. Am. Chem. Soc. 118, 5492.
20. Idzerda Y., D. Trevor, Y. Mark, C. Mary, and S. David (2003), "Template *–constrained synthesis and characterization of nanomagnetic materials*", Nanoscale Science and Engineering Grantees Conference, Dec 16-18.
21. Imai H., Y. Takei, K. Shimizu, M. Matsuda and H. Hirashima (1999), "*Direct preparation of anatase TiO_2 nanotubes in porous alumina membranes*", J. Mater. Chem. 9, 2971.
22. Iwasaki T., Y. Motoi and T. Den (1999), "*Multiwalled carbon nanotubes growth in anodic alumina nanoholes*", Appl. Phys. Lett.75, 2044.
23. Jacobs G., Leann W., Uschi G., Gerald A. T., Dennis E. S. and Burtron H. D. (2003), "*Low temperature water–gas shift: in situ DRIFTS-reaction study of ceria surface area on the evolution of formates on Pt/CeO_2 fuel processing catalysts for fuel cell applications*", Appl. Catal. A, Gen. 252, 107.
24. Jae-Hyun J., J. H. Keum, J. H. Song, and J. S. Kim (2007), "*The fabrication and characterization of organic photovoltaic microcell into the polymer membrane using template synthesis of conductive polymer*", Solar energy materials and solar cells 91, 645-651.
25. Sylvestre J. P., A. V. Kabashin, E. Sacher, and M. Meunier (2005), "*Femtosecond laser ablation of gold in water: influence of the laser-produced plasma on the nanoparticle size distribution*", Appl. Phys. A 80, 753-758.
26. Tabony J. and D. Tob (1990), "*Spatial structures in microtubular solutions requiring a sustained energy source*", Nature 346, 448-451.
27. Tae-Wan K., R. Ryoo, K. P. Gierszal, M. Jaroniec, L. A. Solovyov, Y. Sakamotod and O. Terasakid (2005), "*Characterization of mesoporous carbons synthesized with SBA-16 silica template*", J. Mater. Chem., 15, 1560–1571.
28. Wu C. G. and T. Bein (1994), "*Conducting polyaniline filaments in a mesoporous channel host*", Science, 264, 1757–1759.
29. Wu X. C. and Y. R. Tao (2002), "*Growth of CdS nanowires by physical vapor deposition"* Journal of crystal growth 242, 309-312.
30. Xie G., Z. Wang, L. Guicun, S. Yulong, C. Zuolin, and Z. Zhikun (2007), "*Templated synthesis of metal nanotubes via electroless deposition*", Materials Letters 61,2641-2643.

8/18/2019